Chemical Science

Accepted Manuscript

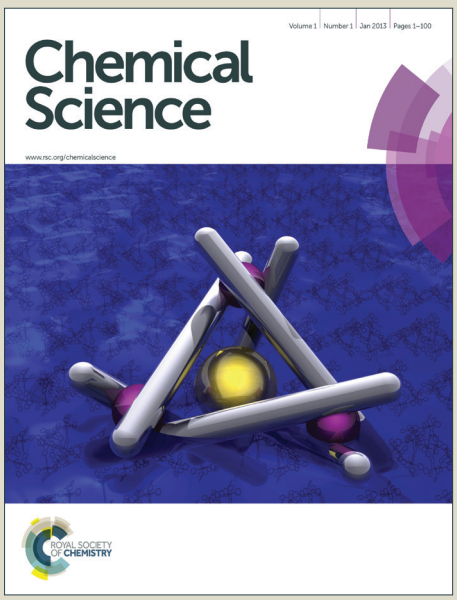

ROYAL SOCIETY OF CHEMISTRY

www.rsc.org/chemicalscience

Journal Name Chemical Science Dynamic Article Links ►

Cite this: DOI: 10.1039/c0xx00000x

www.rsc.org/xxxxxx

ARTICLE TYPE

Ratiometric detection of pH fluctuation in mitochondria with a new fluorescein/cyanine hybrid sensor

Yuncong Chen, Chengcheng Zhu, Jiajie Cen, Yang Bai, Weijiang He,* and Zijian Guo*

Received (in XXX, XXX) Xth XXXXXXXXX 20XX, Accepted Xth XXXXXXXXX 20XX

DOI: 10.1039/b000000x

The homeostasis of mitochondrial pH (pH_m) is crucial for cell physiology. Developing small molecular fluorescent sensor for the ratiometric detection of pH_m fluctuation is highly demanded yet challenging. A ratiometric pH sensor, **Mito-pH**, was constructed by integrating a pH sensitive FITC fluorophore with a pH insensitive hemicyanine group. The hemicyanine group also acts as the mitochondria targeting group due to its lipophilic cationic nature. Besides its positive mitochondria-targetability, this sensor provides two ratiometric pH sensing modes, the dual excitation/dual emission mode (*Dex*/*Dem*) and dual excitation (*Dex*) mode, and its linear and reversible ratiometric response range from pH 6.15 to 8.38 makes this sensor suitable for the practical tracking of pH_m fluctuation in live cells. With this sensor, the stimulated pH_m fluctuation has been successfully tracked in a ratiometric manner *via* both fluorescence imaging and flow cytometry.

Introduction

Different from the acidic organelles such as lysosome and endosome, mitochondria display a slightly basic pH,[1] and the proton gradient established across its inner membrane is essential to sustain the transmembrane potential for ATP production.[2] Therefore, the development of facile and reliable methods to monitor the mitochondrial pH (pH_m) in live cells is highly demanded to understand the mitochondria physiology and pathology. With the great success of intracellular pH (pH_i) fluorescence imaging,[3-6] developing the mitochondria targetable fluorescent pH sensor for pH_m imaging and flow cytometry should be a reliable approach to acquire the in situ pH_m information.[7] Although mammalian pH_i ranges from the slightly acidic in lysosome and endosome (4.7~6.5) to slightly basic in active mitochondria (~8.0), the physiological pH_m deviation is minor but of great significance for the understanding of mitochondria physiology. However, this minor pH_m deviation can be concealed in the case of using turn-on fluorescent sensors since the fluorescence intensity can be affected by local sensor concentration, microenvironment and imaging parameters, etc. Therefore, the ratiometric pH sensors, which offer the possibility of self calibration between dual emission, are more effective and advantageous to reduce the artefacts induced by the above mentioned factors.[8] Although many ratiometric sensors for intracellular pH imaging have been reported,[5,6] the ratiometric sensors for pH_m is still rare and their design remains challenging. The nanoparticle-based design rationale for the ratiometric pH_i sensor has been reported,[6] yet they tend to localize in acidic endocytic compartments other than the slightly basic mitochondria due to their uptake via endocytosis. Besides the successful FRET-based genetically encoded ratiometric pH sensors, which can be selectively expressed in mitochondria,[9] the small molecule ratiometric pH_m senor is especially appealing due to their simple staining procedure, fine reproducibility, and more alternative emission wavelength for imaging.[3] Moreover, small molecular sensors can be more readily endowed with pH sensitivity. Therefore, small molecular sensors are among the most promising approaches to ratiometric pH_m imaging and tracking, and the sensing range from pH 6.50 to pH 8.20 is essential for practical pH_m tracking. Carboxy SNARF-1/AM of no intrinsic mitochondria-targetability has been reported as the very few small molecular sensor for the ratiometric pH_m imaging,[10] its passive mitochondrial accumulation depends on both the higher efflux rate of the dye in cytosol than in mitochondria and the long incubation for ester hydrolysis and efflux equilibrium. It is clear that the small molecular ratiometric pH sensor of intrinsic mitochondria-targetability, which is not reported so far, is more appealing for the positive mitochondria targeting ability.

Herein, we report a small molecular fluorescent sensor, **Mito-pH** (Scheme 1), for ratiometric pH_m imaging. The intrinsic mitochondria targetability of **Mito-pH** was confirmed by co-localization study, which was originated from its lipophilic cationic cyanine moiety. It exhibits the reversible pH sensing ability and a linear response range from pH 6.15 to 8.38. Besides the ratiometric pH_m imaging via confocal microscopy, the general pH_m fluctuation upon stimulations has also been effectively monitored by flow cytometry in a ratiometric manner with this sensor.

Results and discussion

Design and synthesis of Mito-pH

Mito-pH was constructed via hybridizing a pH-sensitive fluorescein (spirolactone form) fluorophore with a pH-insensitive cyanine fluorophore (Scheme 1). Cyanines were well known for their specific intracellular localization in mitochondria due to their lipophilic cationic nature,[11,12] and the cyanine group was incorporated in this sensor as the reference fluorophore for ratiometric sensing as well as the mitochondria targeting group. It is proposed that the non-emissive spiro-xanthen-3-one turns to the emissive fluorescein at high pH, while hemicyanine displays almost stable emission as the reference for ratiometric sensing.

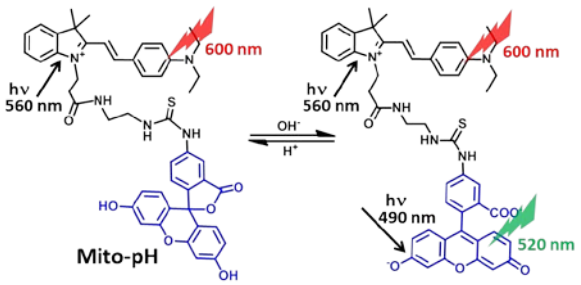

Scheme 1 Chemical structure of **Mito-pH** and the proposed ratiometric pH sensing mechanism.

To prepare this sensor, the cyanine derivative **2** was prepared with a reasonable yield via reacting 1-carboxylethyl-2-methylindolinum with *N,N'*-dimethylaminobenzaldehyde in reflux. The condensation of compound **2** with N^1-Boc-1,2-ethyldiamine followed by TFA treatment resulted in a cyanine derivative with one amino tail (compound **3**). The condensation of compound **3** with fluorescein isothiocyanate (FITC) in the presence of triethylamine afforded the sensor **Mito-pH** (Scheme 2).

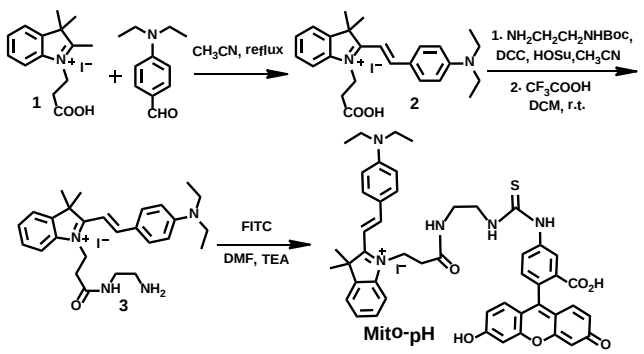

Scheme 2 Synthesis of compound **Mito-pH**.

Spectroscopic study and pH_{app} sensing behaviour of Mito-pH

Due to the precipitation of **Mito-pH** from the PBS buffer of acidic pH when DMSO content is lower than 10%, PBS buffer mixed with 10% DMSO was utilized as the medium to determine the emission spectra of **Mito-pH** at different apparent pH (pH_{app}). As shown in Fig. 1, the emission spectra of **Mito-pH** upon excitation at 490 nm exhibit the characteristic emission band of FITC centered at 520 nm. A distinct enhancement of this band (> 40 fold, Fig. 1a and Fig. S4a) was observed upon increasing medium pH_{app} from 4.85 to 9.65. The high pH_{app} induced fluorescein formation from spiro-xanthen-3-one is responsible for the enhancement. Its emission spectra upon excitation at 560 nm display the characteristic emission band of cyanine centered at 600 nm, which undergoes a decrement of ~30% upon increasing medium pH_{app} from 4.85 to 9.65 (Fig. 1b). The normalized ratio of emission at 520 nm (λ_{ex}, 490 nm) to that at 600 nm (λ_{ex}, 560 nm), F_{520}/F_{600}, increases from 0.023 to 0.99 upon increasing medium pH_{app} from 4.85 to 9.65, and the quantum yield was enhanced from 2.6% to 25%.[13] The apparent pK_a' was determined as 7.33±0.03 via fitting the pH titration profile based on the normalized F_{520}/F_{600} (Fig. 1c).[14] The linear range for the ratiometric response of **Mito-pH** is pH_{app} 6.15 to 8.38 (Fig. S5), in which pH_m lies, favouring the practical pH_m tracking. This ratiometric pH sensing behaviour is originated from the different pH sensing behaviours of the two hybridized fluorophores, FITC and cyanine. In addition, the enhanced F_{520}/F_{600} value of **Mito-pH** at pH_{app} 9.00 can be recovered to the original F_{520}/F_{600} value at pH_{app} 5.00, and this reversible ratiometric pH sensing ability can be retained for at least 5 cycles in the pH_{app} range from 5.00 to 9.00 (Fig. 1d).

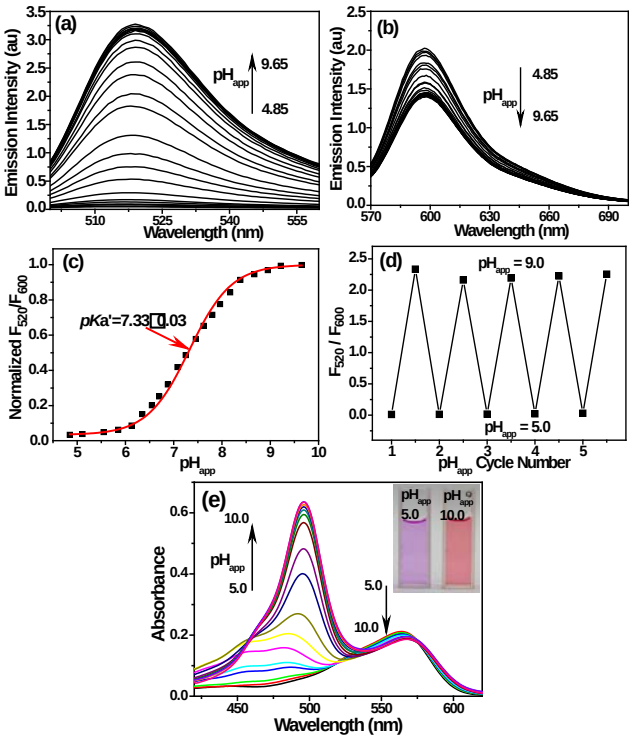

Fig. 1 Emission spectra of 10 μM **Mito-pH** in DMSO-PBS buffer (1:9, v/v) solutions of different pH_{app} values determined upon excitation at 490 nm (a) and 560 nm (b). (c) The related pH titration profile (■) based on the normalized emission ratio F_{520}/F_{600} calculated from (a) and (b) and the fitting profile (red line). (d) Emission ratio F_{520}/F_{600} of 10 μM **Mito-pH** in the same medium determined in the consecutive pH_{app} cycles. (e) Absorption spectra of **Mito-pH** (10 μM) in the same media of different pH_{app}. Inset: photograph of the solutions at different pH in ambient light.

The absorption spectrum of **Mito-pH** at pH_{app} 9.00 shows a major absorption band centered at 490 nm which can be assigned as the FITC absorption band, and a minor band centered at 565 nm which can be assigned as the cyanine absorption band. However, the absorption spectrum at low pH_{app} (< 5.00), shows only the cyanine band due to the absorption nature of FITC spiro-form. The FITC band appears gradually and undergoes a significant enhancement with the medium pH_{app} increasing from 5.00 to 10.00, while the cyanine band remains almost stable. This

ratiometric response can be clearly visualized from the distinct colour change of **Mito-pH** solution from purple to pink during the titration process (Fig. 1e).

On the other hand, the excitation spectra of **Mito-pH** at different pH demonstrate that the excitation maximum at 560 nm at pH_{app} 5.02 can be shifted to 490 nm at pH_{app} 8.55. The ratio of emission at 600 nm upon excitation at 560 nm to that upon excitation at 490 nm, F_{490}/F_{560}, shows a linear enhancement with the medium pH_{app} increasing from 6.04 to 8.25 (Fig. 2). This additional dual excitation ratiometric pH sensing ability implies **Mito-pH** is able to offer two ratiometric imaging modes, the dual excitation/dual emission (*Dex/Dem*) mode and the dual excitation (*Dex*) mode. Therefore, this sensor possesses the advantage of the flexibility to match the laser/filter sets of microscopes and flow cytometer.

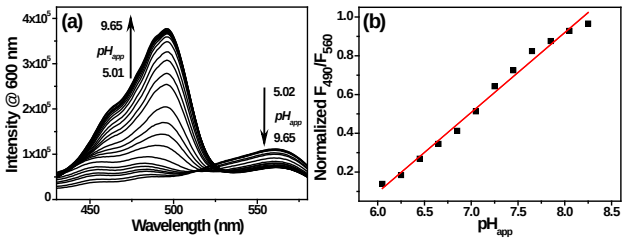

Fig. 2 (a) Excitation spectra of 10 μM **Mito-pH** in DMSO-PBS buffer (1:9, v/v) solutions with pH ranging from 5.02 to 9.65. λ_{em}, 600 nm. (b) Linear fitting (red line) of the related F_{490}/F_{560} profile (■) of **Mito-pH**. F_{490}/F_{560} is the normalized ratio of emission at 600 nm upon excitation at 490 nm to that upon excitation at 560 nm.

The ratiometric fluorescent response of **Mito-pH** to different biological species was also investigated in PBS buffer (pH 7.40). The emission ratio F_{520}/F_{600} exhibits the negligible change in the presence of essential metal ions (K^+, Ca^{2+}, Na^+, Mg^{2+}, 10 mM; Zn^{2+}, Cu^{2+}, Fe^{2+}, Fe^{3+}, 10 μM) and biological related redox chemicals (GSH, 10 mM; Cys, 1 mM; H_2O_2, ClO^-, NO, O_2^-, ·OH, 100 μM), demonstrating the specific ratiometric response of **Mito-pH** solely to pH_{app} (Fig. 3). All these suggest **Mito-pH** might be a suitable candidate for ratiometric intracellular pH imaging.

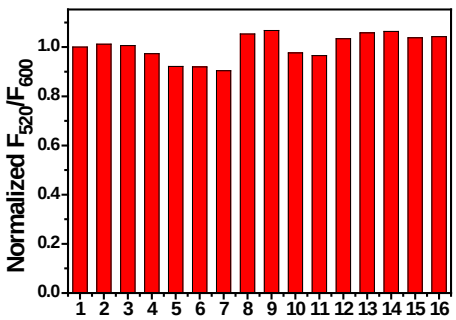

Fig. 3 Normalized emission ratio, F_{520}/F_{600}, of 10 μM **Mito-pH** in PBS solution (10 mM, pH 7.40, 10% DMSO-H_2O, v/v) in the presence of different metal ions and biological redox species. 1, blank; 2, K^+; 3, Na^+; 4, Ca^{2+}; 5, Mg^{2+} (2-5: 10 mM); 6, Zn^{2+}; 7, Cu^{2+}; 8, Fe^{2+}; 9, Fe^{3+} (6-9: 10 μM); 10, GSH (10 mM); 11, Cys (1 mM); 12, H_2O_2 (100 μM); 13, ClO^- (100 μM); 14, NO (100 μM); 15, O_2^- (100 μM); 16, ·OH (100 μM). F_{520}/F_{600}, the ratio of emission at 520 nm (λ_{ex}, 490 nm) to that at 600 nm (λ_{ex}, 560 nm).

Ratiometric pH_m imaging behaviour of Mito-pH

The intrinsic mitochondria-targetability of **Mito-pH** was investigated in live MCF-7 cells at pH 7.40 and 8.50, respectively. The **Mito-pH** stained cells (10 μM, 30 min, 25°C) were co-stained further with the commercial available mitochondria dye Mito-Tracker Deep Red 633 (1 μM, 30 min) in culture medium, and the pH_i was regulated by the following incubation with high K^+ buffers of different pH containing nigericin (10 μM), an H^+/K^+ ionophore to homogenize the intra- and extracellular pH. The imaging results show that green image for **Mito-pH** channel obtained upon excitation at 543 nm is almost identical to the red image for Mito-Tracker channel obtained upon excitation at 633 nm (Fig. 4 and Fig. S6). The overlay between the fluorescence images of **Mito-pH** and Mito-Tracker Deep Red 633 discloses the Pearson's correction coefficient of 0.96 at pH 7.40 and 0.93 at pH 8.50, suggesting the pH-independent mitochondria-targeting ability of **Mito-pH**. With this intrinsic mitochondria-targetability, the mitochondria staining equilibrium staining can be acquired much quicker by **Mito-pH** than that by carboxy SNARF-1/AM, which depends on the time-consuming dye ester hydrolysis and efflux process.

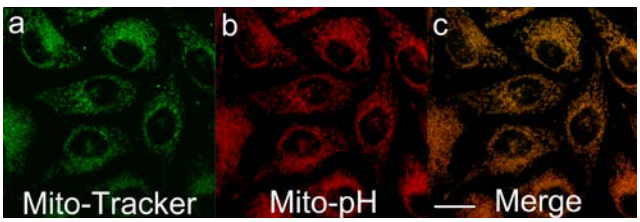

Fig. 4 Pseudo-colour confocal fluorescence images of MCF-7 cells incubated firstly with DMEM containing **Mito-pH** (10 μM, 60 min) and Mito-Tracker Deep Red 633 (1 μM, 30 min) at 25°C, followed by incubation with high K^+ buffers (30 mM NaCl, 120 mM KCl, 1 mM $CaCl_2$, 0.5 mM $MgSO_4$, 1 mM NaH_2PO_4, 5 mM glucose, 20 mM HEPES, and 20 mM NaOAc) of pH 7.40 in the presence of 10.0 μM nigericin. (a) Fluorescence image obtained with the band path 660-750 nm upon excitation at 633 nm (Mito-Tracker channel); (b) fluorescence image obtained with the band path 560-640 nm upon excitation at 543 nm (**Mito-pH** channel); (c) overlay of (a) and (b). Scale bar: 20 μm.

With the confirmed intrinsic mitochondria-targetability, **Mito-pH** was further studied for its ratiometric pH_m imaging ability via a *Dex/Dem* mode. In this study, the intracellular pH calibration was carried out in MCF-7 cells using a standard procedure. MCF-7 cells were incubated first with culture medium containing 10 μM **Mito-pH** for 30 min followed by the further incubation with high K^+ buffers of different pH containing also nigericin (10 μM). As shown in Fig. 5a, the green channel images (green channel: λ_{ex} 488 nm, band path 500-550 nm for FITC) display a gradually enhanced emission of fluorescein upon increasing pH from 6.50 to 8.50, while the red channel images (red channel: λ_{ex} 543 nm, band path 560-650 nm for hemicyanine) show generally a slightly decreased fluorescence of hemicyanine. Moreover, the ratio images obtained via mediating the green with the related red channel images at the same pH by the program for ratiometric imaging show that the average ratio of green channel emission to the red channel one was enhanced linearly with the intracellular pH i.e. pH_m in this experiment (Fig. 5b). All these confirm the ratiometric pH_m imaging ability of **Mito-pH** via the *Dex/Dem* mode. With the ratiometric imaging calibration curve for pH_m (Fig. 5b), the ratiometric imaging of MCF-7 cells incubated with neutral PBS buffer without nigericin disclosed that the pH_m of

intact cells is 7.9 ± 0.1, which is in agreement with the results determined using the genetically encoded fluorescent pH sensor.[4a,7]

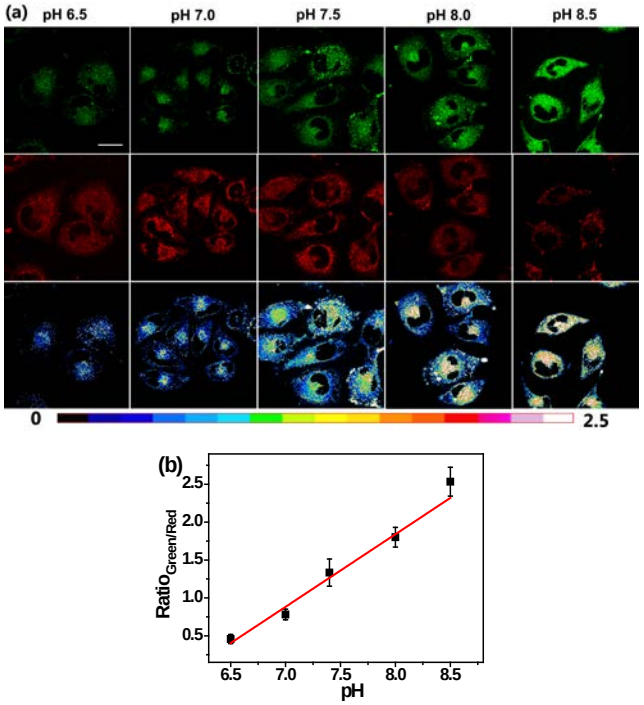

Fig. 5 (a) Ratiometric imaging of MCF-7 cells stained by **Mito-pH** (10 μM in DEME with 0.1% DMSO, 30 min, 25°C) upon further incubation with high K^+ buffers (30 mM NaCl, 120 mM KCl, 1 mM $CaCl_2$, 0.5 mM $MgSO_4$, 1 mM NaH_2PO_4, 5 mM glucose, 20 mM HEPES, and 20 mM NaOAc) of different pH (6.50-8.50) in the presence of 10.0 μM nigericin. The green channel images (first row) were collected with a band path of 500-550 nm upon excitation at 488 nm, the red channel images (second row) were collected with a band path of 560-650 nm upon excitation at 543 nm. Pseudo-colour ratio images (third row) were obtained by mediating the green channel image with the red channel at the same pH. The colour strip is the ratio bar. Scale bar: 20 μm. (b) Calibration curve of pH_m based on the imaging results shown in (a).

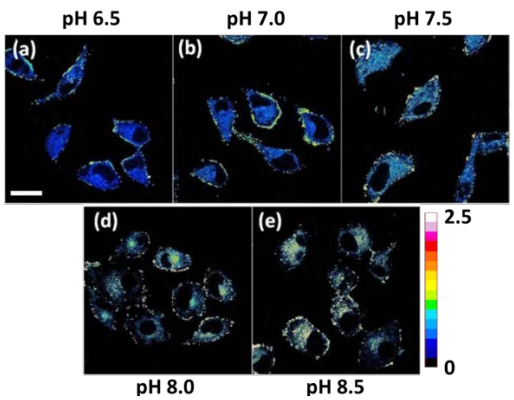

Fig. 6 Pseudo-colour ratio images of MCF-7 cells stained by **Mito-pH** (10 μM in DEME with 0.1% DMSO, 30 min, 25°C) upon further incubation with high K^+ buffers (30 mM NaCl, 120 mM KCl, 1 mM $CaCl_2$, 0.5 mM $MgSO_4$, 1 mM NaH_2PO_4, 5 mM glucose, 20 mM HEPES, and 20 mM NaOAc) of different pH (6.50-8.50) in the presence of 10.0 μM nigericin. The imaging was carried out with a dual excitation mode (channel 1: λ_{ex}, 488 nm; channel 2: λ_{ex}, 543 nm; band path for both channel is 560-650 nm) and the ratiometric images were obtained by mediating the channel 1 image with the related channel 2 image at the same pH. Scale bar: 20 μm.

As mentioned above that **Mito-pH** displays still the ratiometric sensing ability for pH via the *Dex* mode. Therefore the ratiometric pH_m imaging ability was also investigated using the dual excitation imaging mode (Channel 1: λ_{ex1}, 488 nm; Channel 2: λ_{ex2}, 543 nm; band path 560-650 nm) in MCF-7 cells treated in the same way shown in *Dex/Dem* imaging mode. The ratiometric images were obtained via mediating the image obtained from channel 1 with the related channel 2 image at the same pH. These *Dex* ratiometric images display also the linearly enhanced average ratio value inside the cells with the pH of the nigericin-containing high K^+ buffer for cell incubation being raised from 6.50 to 8.50 (Fig. 6). This result demonstrates also the ratiometric pH_m imaging ability of **Mito-pH** via the *Dex* imaging mode.

Ratiometric flow cytometry for pH_m with Mito-pH

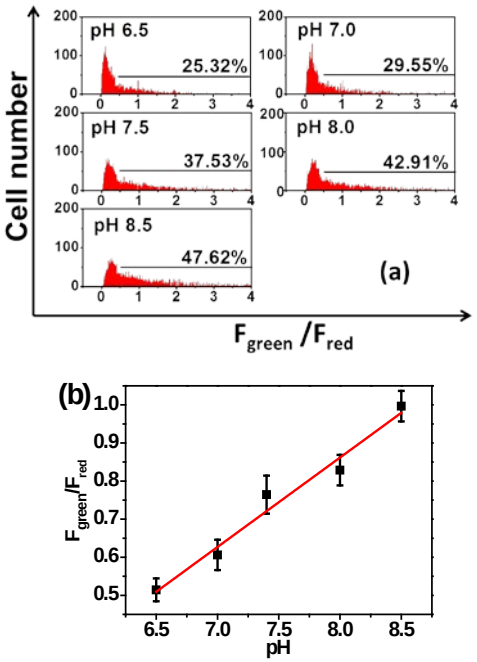

Fig. 7 (a) pH_m flow cytometry of **Mito-pH** stained MCF-7 cells upon incubation with high K^+ buffers (30 mM NaCl, 120 mM KCl, 1 mM $CaCl_2$, 0.5 mM $MgSO_4$, 1 mM NaH_2PO_4, 5 mM glucose, 20 mM HEPES, and 20 mM NaOAc) of different pH values (6.50-8.50) in the presence of 10.0 μM nigericin. Y-axis is the cell number, X-axis is the average F_{green}/F_{red} ratio of cells. The percentage shown for each tested pH value indicates the proportions of cells with F_{green}/F_{red} higher than 0.5. Green channel: filter 530 ±15 nm, λ_{ex}, 488 nm; red channel: filter 610 ± 10 nm, λ_{ex}, 561 nm. (b) Average F_{green}/F_{red} ratio (■) of the **Mito-pH** stained MCF-7 cells at different pH according to the data shown in (a) and it linear fitting (red line).

The tracking of pH_m in a large number of cells is crucial for understanding the general behaviors of mitochondria, and the successful ratiometric pH_m imaging with **Mito-pH** inspires us to explore the possibility of ratiometric pH_m detection with this sensor via flow cytometry, which should offer more reliable pH_m due to the massive cells other than the limited cell numbers in fluorescence imaging. The pH_m flow cytometry with this sensor was investigated in MCF-7 cells with a *Dex*/*Dem* mode. Therefore, the **Mito-pH** stained cells were detected by recording the green channel emission (detection path 530 ±15 nm, λ_{ex}, 488 nm) and the red channel emission (detection path 610 ± 10 nm, λ_{ex}, 561 nm) respectively. The cell distribution pattern was

analysed via calculating the emission ratio of green channel to red channel (F_{green}/F_{red}). The results demonstrate that the number of cells with F_{green}/F_{red} higher than 0.5 increases distinctly upon increasing the incubation media pH from 6.50 to 8.50 (Fig. 7a). Moreover, the average F_{green}/F_{red} ratio displays also a linear enhancement with the pH values (Fig. 7b). The similar ratiometric pH response of **Mito-pH** in flow cytometry and confocal imaging confirms the effectiveness of this sensor to monitor pH_m in live cells via the ratiometric manner.

Tracking the stimulated pH_m fluctuation by Mito-pH via fluorescence imaging and flow cytometry

The practical ratiometric pH_m imaging ability of **Mito-pH** was further applied in monitoring pH_m fluctuation upon different stimulation (Fig. 8). The **Mito-pH** stained MCF-7 cells were incubated with carbonyl cyanide *m*-chlorophenylhydrazone (CCCP), which is a protonophore to uncouple the mitochondrial proton gradient across the inner membrane.[4a] The ratiometric imaging via *Dex*/*Dem* mode displays an instant and rapid drop of pH_m from 7.9 ± 0.1 to 7.2 ± 0.1 in the initial 5 min of CCCP incubation, and the pH_m tends to be stabilized at 7.1 ± 0.1 after 13 min incubation (Fig. 8d). This result suggests the CCCP-induced damage to oxidative phosphorylation might be correlated to the impairing of mitochondria proton gradient. Since most of the intracellular oxidative stress occurs in mitochondria, exploring the influence of oxidative stress on pH_m should be helpful to understand the role of pH_m in electron transport chain and oxidative phosphorylation. Therefore, the pH_m fluctuation upon incubation with phorbol myristate acetate (PMA, 5μg/mL), which stimulates the generation of intracellular reactive oxygen species (ROS),[15] was monitored via ratiometric imaging using **Mito-pH** as the imaging agent. The imaging demonstrates a rapid pH_m drop from 7.9 ± 0.1 to 6.8 ± 0.1 upon incubation with PMA. The temporal pH profile indicates clearly that the mitochondrial acidification stimulated by the PMA-induced oxidative stress can be finished within 5 min (Figure 8d), and this mitochondria acidification might be attributed to the hydroxyl radicals triggered by PMA from the Fenton reaction between H_2O_2 and Fe^{2+}.[16]

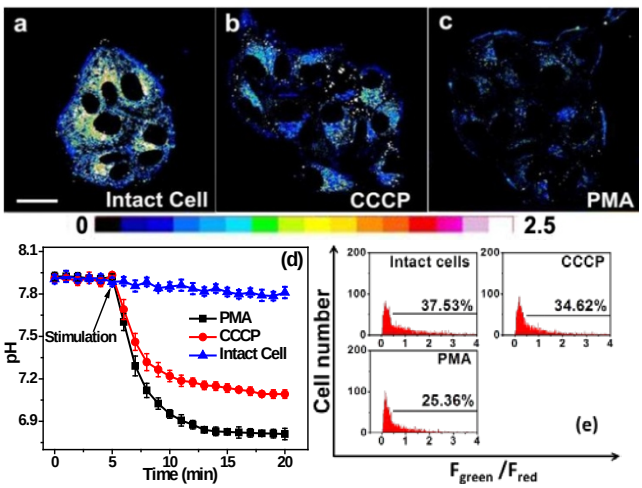

Fig. 8 (a-c) Ratiometric images of **Mito-pH**-loaded MCF-7 cells in the presence of different stimulation agents. (a) Image of intact cells; (b) image of cells incubated with 10 μM CCCP; (c) image of cells incubated with 5 μg/mL PMA. Scale bar: 20 μm. Imaging condition is same as that shown in Fig. 5. (d) The calculated temporal pH_m profiles of MCF-7 cells shown in (a-c) based on the calibration curve shown in Fig 5b. (e) pH_m flow cytometry of **Mito-pH** stained MCF-7 cells after 30 min of stimulation with 10 μM CCCP or 5 μg/mL PMA. Y-axis is the cell number, X-axis is the average F_{green}/F_{red} ratio. The percentage shown in each lane indicates the proportions of cells with F_{green}/F_{red} ratio higher than 0.5. Green channel: filter 530 ±15 nm, λ_{ex}, 488 nm; red channel: filter 610 ± 10 nm, λ_{ex}, 561 nm.

The pH_m deviation in MCF-7 cells upon stimulation with CCCP and PMA has also been determined *via* ratiometric flow cytometry with **Mito-pH**. The results demonstrate that the cell number of F_{green}/F_{red} higher than 0.5 decrease distinctly after 30 min of incubation in both cases. The average pH_m after CCCP incubation is ~7.20, while that after PMA incubation is ~6.60 according the calibration curve shown in Fig. 7b. This result implies that the improper reduction of O_2 in the electron transport chain results in ROS formation to trigger the pH_m drop, disfavouring the oxidative phosphorylation.

Conclusions

Hybridizing pH sensitive FITC with pH insensitive cyanine led to the first small molecular ratiometric pH sensor of intrinsic mitochondria targetability. The fluorescent ratiometric response achieved via the self-calibration with cyanine reference leads to two different ratiometric pH imaging modes: the *Dex*/*Dem* mode and *Dex* mode, which offer more flexibility in pH_m imaging. The linear ratiometric pH response range from pH 6.15 to 8.38, the reversible pH sensing ability, the cell membrane permeability, and the mitochondria targeting nature make this sensor especially suitable for the practical tracking of pH_m fluctuation in live cells via both ratiometric imaging and flow cytometry. Although the ratiometric imaging modes of **Mito-pH** is not so excellent as that of single excitation mode in the tracking of very rapid physiological process, the technological progress in confocal microscope and flow cytometer can provide the *Dex*/*Dem* mode with the promoted scan rate and convenience similar to the single excitation mode, just as shown in the successful pH_m tacking upon PMA and CCCP stimulations. Moreover, this work provides not only a powerful imaging agent for pH_m but also ab example of fluorophore hybridizing strategy to construct ratiometric pH_m sensor, offering more accurate pH_m detection to clarify the physiological processes inside mitochondria.

Experimental section

Materials and general methods

All the solvents used in sensor preparation were of analytic grade, while the solvents used in spectroscopic study were of HPLC grade, and the purified water obtained from Millipore (>18.2 MΩ) was used for this study. The stock solutions of all the tested compounds were prepared from NaCl, KCl, $MgCl_2$, $CaCl_2$, $ZnCl_2$, $CuCl_2$, $FeCl_2$, $FeCl_3$, cysteine, glutathione with the purified water. ROS and RNS were prepared according to the reported procedures.[17] The ^1H NMR and ^{13}C NMR spectra were recorded on Bruker DRX-500 with TMS as internal reference. High resolution mass spectrometric data were determined with an Agilent 6540Q-TOF HPLC-MS spectrometer. Fluorescence spectra were determined on a FluoroMax-4 spectrofluorometer with 5 nm slit for both excitation and emission. Absorption

spectra were recorded with a Shimadzu UV-3100 spectrophotometer. All media pH measurements were accomplished by a Model PHS-3C meter.

Confocal fluorescence imaging

MCF-7 cells were cultured in DMEM (Dulbecco's modified Eagle's medium) supplemented with 10% FBS (fetal bovine serum) in an atmosphere of 5% CO_2 and 95% air at 37 °C. The ratiometric imaging of MCF-7 cells was imaged by laser scanning confocal fluorescence microscope (Zeiss LSM710).

For mitochondria co-localization study, MCF-7 cells were stained firstly at 25°C with the culture media (DMEM) containing 10 μM **Mito-pH** and 0.1% DMSO for 30 min, then 1 μM Mito-Tracker Deep Red 633 was added into the medium for an additional incubation (30 min). After removing the culture medium, the cells were further incubated with high K^+ buffers (30 mM NaCl, 120 mM KCl, 1 mM $CaCl_2$, 0.5 mM $MgSO_4$, 1 mM NaH_2PO_4, 5 mM glucose, 20 mM HEPES, and 20 mM NaOAc) of pH 7.40 or 8.50 in the presence of 10.0 μM nigericin. The fluorescence images were obtained respectively with band path 560-640 nm upon excitation at 543 nm (**Mito-pH**) and band path 660-750 nm upon excitation at 633 nm (Mito-Tracker).

For the ratiometric pH_m calibration in live MCF-7 cells, the cells were stained with DMEM containing **Mito-pH** (10 μM) and 0.1% DMSO for 30 min at 25°C, then the cells were further incubated (30 min) with high K^+ buffers (30 mM NaCl, 120 mM KCl, 1 mM $CaCl_2$, 0.5 mM $MgSO_4$, 1 mM NaH_2PO_4, 5 mM glucose, 20 mM HEPES, and 20 mM NaOAc) of different pH values (6.50-8.50) in the presence of 10.0 μM nigericin. For the *Dex*/*Dem* ratiometric imaging mode, the green and red channel images were collected respectively with the band path of 500-550 nm upon excitation at 488 nm and the band path of 560-650 nm upon excitation at 543 nm. Pseudo-colour ratiometric images were obtained by mediating the green channel image with the red channel at the same pH. The pH_m calibration was obtained finally based on the average intracellular ratio values shown in the ratiometric images. For the *Dex* ratiometric imaging mode, the fluorescence images from channels 1 and 2 were collected with a band path of 560-650 nm upon excitation respectively at 488 (channel 1) and 543 (channel 2) nm, and the ratiometric images were obtained via mediating the channel 1 image with the related channel 2 image at the same pH.

For the ratiometric tracking of pH_m in MCF-7 cells upon CCCP or PMA stimulation, the cells were stained with DEME containing **Mito-pH** (10 μM) for 30 min at 25°C. After **Mito-pH** incubation, the cells were incubated respectively with CCCP (10 μM) and PMA (5 μg/mL) for 15 min, and fluorescence images were obtained every 1 min for both green and red channels with the *Dex*/*Dem* mode. The pH values at different time were calculated with the average ratio values obtained from the related ratiometric images according to the pH_m calibration shown in Fig. 5b.

Ratiometric flow cytometric study

The flow cytometry tests were finished with BD FACS AriaII using the *Dex*/*Dem* ratiometric mode (green channel: filter 530 ±15 nm, λ_{ex}, 488 nm; red channel: filter 610 ± 10 nm, λ_{ex}, 561 nm). MCF-7 cells were stained with the same method shown in ratiometric imaging. Then the stained MCF-7 cells were incubated further with high K^+ buffers (30 mM NaCl, 120 mM KCl, 1 mM $CaCl_2$, 0.5 mM $MgSO_4$, 1 mM NaH_2PO_4, 5 mM glucose, 20 mM HEPES, and 20 mM NaOAc) of different pH values (6.50-8.50) in the presence of 10.0 μM nigericin for an additional 30 min. After trypsinization with 0.25% pancreatin, all the cells were cooled with ice before test. The fluorescence data were collected respectively from the green channel and red channels. The ratio of F_{green}/F_{red} was calculated to give the pH_m calibration in flow cytometric study. For the stimulated pH_m fluctuation monitoring, the fluorescence data were collected similarly after the **Mito-pH** stained MCF-7 cells were treated with CCCP (10 μM) or PMA (5 μg/mL) for 30 min. Then, the pH_m was obtained according to the detected average F_{green}/F_{red} ratio based on the pH_m calibration for flow cytometry shown in Fig. 7b.

Synthesis and characterization

Synthesis of 2: Compound **1** (3.6 g, 10 mmol) and 4-(dimethylamino)benzaldehyde (1.8 g, 10 mmol) were dissolved in 20 mL CH_3CN, and the reaction mixture was refluxed with stirring for 12 h and then evaporated *in vacuo*. The residue was purified by column chromatography on silica gel (CH_2Cl_2/ MeOH, 20:1 v/v) to give **2** (3.0 g) as dark purple solid. Yield, 59%. ^1H NMR (500 MHz, CD_3OD, *ppm*): δ 1.30 (*t*, *J* = 7.5 Hz, 6H), 1.82 (*s*, 6H), 2.96 (*t*, *J* = 7.5 Hz, 2H), 3.64 (*q*, *J* = 6.7 Hz, 4H), 4.76 (*t*, *J* = 7.5 Hz, 2H), 6.93 (*d*, *J* = 10.0 Hz, 2H), 7.30 (*d*, *J* = 15 Hz, 1H), 7.49 (*t*, *J* = 7.5 Hz, 1H), 7.56 (*t*, *J* = 10.0 Hz, 1H), 7.64 (*m*, *J* = 8.8 Hz, 2H), 7.97 (*d*, 10.0 Hz, 2H), 8.33 (*d*, *J* = 15.0 Hz, 1H). ESI-HRMS (m/z, positive mode): calcd. 391.2386, found 391.2381 for $[M-I]^+$.

Synthesis of 3: Compound **2** (500 mg, 1 mmol), DCC (250 mg, 1.2 mmol), and HOSu (140 mg, 1.2 mmol) were mixed in 25 mL CH_3CN, and then *tert*-butyl(2-aminoethyl)carbamate (160 mg, 1 mmol) was added into the mixture. The solution was stirred at room temperature for 6 hours. After removing the solvent *in vacuo*, the residue was purified by column chromatography on silica gel (CH_2Cl_2/ MeOH, 10:1 v/v) to give a purple solid. The resulted solid (330 mg, 0.5 mmol) was dissolved in 5 mL CH_2Cl_2, then 3 mL of TFA was added dropwise into the solution. The mixture was stirred at room temperature for 1 hour. The solvent and TFA were removed *in vacuo*, and the resulted residue was purified by column chromatography on silica gel (CH_2Cl_2/ MeOH, 9:1 v/v) to give **3** (250 mg). Yield, 54%. ^1H NMR (500 MHz, MeOD, ppm):δ 1.30 (*t*, *J* = 7.5 Hz, 6H), 1.83 (*s*, 6H), 2.06 (*s*, 2H), 2.97 (*t*, *J* = 7.5 Hz, 2H), 3.64 (*q*, *J* = 8.3 Hz, 4H), 4.76 (*t*, *J* = 7.5 Hz, 2H), 6.93 (*d*, *J* = 10.0 Hz, 2H), 7.31 (*d*, *J* = 15.0 Hz, 1H), 7.49 (*t*, *J* = 7.5 Hz, 1H), 7.56 (*t*, *J* = 7.5 Hz, 1H), 7.65 (*q*, *J* = 8.3 Hz, 2H), 7.96 (*d*, *J* = 5.0, 2H), 8.33 (*d*, *J* = 15.0 Hz, 1H). ^{13}C NMR (126 MHz, CD_3OD, ppm): δ 154.84, 128.90, 127.49, 122.56, 113.29, 112.48, 103.98, 44.97, 41.93, 40.10, 36.67, 33.67, 26.50, 11.95 ppm. ESI-HRMS (m/z, positive mode): calcd. 433.2967, found 433.2971 for $[M-I]^+$.

Synthesis of Mito-pH: Compound **3** (560 mg, 1.0 mmol), FITC (389 mg, 1.0 mmol), and triethylamine (1 mL) were dissolved in 15 mL DMF, and the mixture was stirred at room temperature under N_2 for 4 hours. The solvent were removed *in vacuo*, and the resulted residue was purified by column chromatography on silica

gel (CH_2Cl_2/ MeOH, 8:1 v/v) to give **Mito-pH** (120 mg). Yield, 13%. ^{1}H NMR (500 MHz, *d*-DMSO, ppm):δ 1.16 (*t*, *J* = 7.5 Hz, 6H), 1.76 (*s*, 6H), 2.73 (*t*, *J* = 5.0 Hz, 2H), 3.19 (*d*, *J* = 10.0 Hz, 2H), 3.54 (*q*, *J* = 6.7 Hz, 6H), 4.77 (*t*, *J* = 5.0, 2H), 6.58 (*q*, *J* = 6.7 Hz, 4H), 6.70 (*s*, 2H), 6.87 (*d*, *J* = 10.0 Hz, 2H), 7.16 (*d*, *J* = 5.0 Hz, 2H), 7.30 (*d*, *J* = 15.0 Hz, 1H), 7.45 (*t*, *J* = 7.5 Hz, 1H), 7.53 (*t*, *J* = 7.5 Hz, 1H), 7.69 (*d*, *J* = 10.0 Hz, 1H), 7.77 (*t*, *J* = 10.0 Hz, 2H), 8.07 (*d*, *J* = 10.0 Hz, 2H), 8.32 (*t*, *J* = 7.5, 2H), 8.40 (*s*, 1H), 8.54 (*s*, 1H) ppm. ^{13}C NMR (126 MHz, *d*-DMSO, ppm):δ13.01, 27.03, 34.21, 38.43, 42.48, 43.10, 44.92, 51.04, 102.73, 105.05, 110.19, 112.52, 113.08, 113.88, 116.34, 122.63, 123.14, 124.42, 126.99, 127.67, 129.13, 129.42, 131.98, 137.33, 141.49, 142.05, 142.99, 147.29, 149.54, 152.37, 153.16, 154.80, 160.05, 169.07, 169.86, 179.93, 181.18. ESI-HRMS (m/z, positive mode): calcd. 822.3325, found 822.3322 for $[M-I]^+$.

Acknowledgements

We thank the National Basic Research Program of China (No. 2015CB856300 and 2011CB935800) and National Natural Science Foundation of China (No. 21271100, 10979019 and 21131003) for financial support. Y. Chen was supported by the Program A for outstanding PhD candidate of Nanjing University (No. 201301A05).

Notes and references

State Key Laboratory of Coordination Chemistry, Coordination Chemistry Institute, School of Chemistry and Chemical Engineering, Nanjing University. Hankou Road No.22, Nanjing 210093, PR China . Fax: +86-25-83314502; Tel: +86-25-83597066; E-mail: heweij69@nju.edu.cn; zguo@nju.edu.cn

† Electronic Supplementary Information (ESI) available: [characterization of **Mito-pH**, emission spectra and photograph of **Mito-pH** solutions, linear fitting of ratiometric ressponse, co-localization images at pH 8.50]. See DOI: 10.1039/b000000x/

‡ Footnotes should appear here. These might include comments relevant to but not central to the matter under discussion, limited experimental and spectral data, and crystallographic data.

1 J. R. Casey, S. Grinstein and J. Orlowski, *Nat. Rev. Mol. Cell Biol.*, 2010, **11**, 50–61.

2 (a) P. Mitchell, *Boil. Rev.*, 1966, **41**, 445–501; (b) P. Mitchell and J. Moyle, *Nature*, 1967, **213**, 137–139.

3 J. Han, K. Burgess, *Chem. Rev.*, 2010, **110**, 2709–2728.

4 (a) J. Llopis, J. M. McCaffery, A. Miyawaki, M. G. Farquhar and R. Y. Tsien, *Proc.Natl. Acad. Sci. U. S. A.*, 1998, **95**, 6803–6808; (b) F. Galindo, M. I. Burguete, L. Vigara, S. V. Luis, N. Kabir, J. Gavrilovic and D. A. Russell, *Angew. Chem. Int. Ed.*, 2005, **44**, 6504 –6508; (c) Y. Urano, D. Asanuma, Y. Hama, Y. Koyama, T. Barrett, M. Kamiya, T. Nagano, T. Watanabe, A. Hasegawa, P. L. Choyke and H. Kobayashi, *Nat. Med.*, 2009, **15**, 104-109; (d) M. Yang, Y. Song, M. Zhang, S. Lin, Z. Hao, Y. Liang, D. Zhang and P. R. Chen, *Angew. Chem. Int. Ed.*, 2012, **51**, 7674 –7679; (e) B. Tang, F. Yu, P. Li, L. Tong, X. Duan, T. Xie and X. Wang, *J. Am. Chem. Soc.*, 2009, **131**, 3016–3023; (f) A. V. Romero, N. Kielland, M. J. Arévalo, S. Preciado, R. J. Mellanby, Y. Feng, R. Lavilla and M. Vendrell, *J. Am. Chem. Soc.*, 2013, **135**, 16018−16021.

5 (a) T. J. Rink, R. Y. Tsien and T. J. Pozzan, *J. Cell Biol.*, 1982, **95**, 189-196; (b) S. Matsuyama, J. Llopis, Q. L. Deveraux, R. Y. Tsien and J. C. Reed, *Nat. Cell Biol.*, 2000, ***2***, 318-325; (c) J. Han, A. Loudet, R. Barhoumi, R. C. Burghardt and K. Burgess, *J. Am. Chem. Soc.*, 2009, **131**, 1642–1643; (d) T. Myochin, K. Kiyose, K. Hanaoka, H. Kojima, T. Terai and T. Nagano, *J. Am. Chem. Soc.*, 2011, **133**, 3401–3409; (e) H. J. Park, C. S. Lim, E. S. Kim, J. H. Han, T. H. Lee, H. J. Chun and B. R. Cho, *Angew. Chem. Int. Ed.*, 2012, **51**, 2673 – 2676; (f) M. H. Lee, J. H. Han, J. H. Lee, N. Park, R. Kumar, C. Kang and J. S. Kim, *Angew. Chem. Int. Ed.*, 2013, **53**, 6206–6209; (g) H. J. Kim, C. H. Heo and H. M. Kim, *J. Am. Chem. Soc.*, 2013, **135**, 17969−17977.

6 (a) P. T. Snee, R. C. Somers, G. Nair, J. P. Zimmer, M. G. Bawendi and D. G. Nocera, *J. Am. Chem. Soc.*, 2006, **128**, 13320-13321; (b) H. Peng, J. A. Stolwijk, L. Sun, J. Wegener and O. S. Wolfbeis, *Angew. Chem. Int. Ed.*, 2010, **49**, 4246–4249; (c) W. Shi, X. Li and H. Ma, *Angew. Chem. Int. Ed.*, 2012, **51**, 6432–6435; (d) M. J. Marín, F. Galindo, P. Thomas and D. A. Russell, *Angew.Chem. Int. Ed.*, 2012, **51**, 9657–9661; (e) J. Lei, L. Wang and J. Zhang, *Chem. Commun.*, 2010, **46**, 8445–8447; (f) S. Wu, Z. Li, J. Han and S. Han, *Chem. Commun.*, 2011, **47**, 11276–11278; (g) G. Sun, H. Cui, L. Y. Lin, N. S. Lee, C. Yang, W. L. Neumann, J. N. Freskos , J. J. Shieh , R. B. Dorshow and K. L. Wooley, *J. Am. Chem. Soc.*, 2011, **133**, 8534–8543; (h) S. Chen, Y. Hong, Y. Liu, J. Liu, C. W. T. Leung, M. Li, R. T. K. Kwok, E. Zhao, J. W. Y. Lam, Y. Yu and B. Z. Tang, *J. Am. Chem. Soc.*, 2013, **135**, 4926−4929; (i) X. Wang, R. J. Meier and O. S. Wolfbeis, *Angew. Chem. Int. Ed.*, 2013, **52**, 406–409; (j) Y. Chiu, S. Chen, J.-H. Chen, K.-J. Chen, H.-L. Chen and H.-W. Sung, *ACS Nano*, 2010, **4**, 7467−7474; (k) Q. Wan, S. Chen, W. Shi, L. Li and H. Ma, *Angew. Chem. Int. Ed.*, 2014, **53**, 10916–10920.

7 (a) P. Li, H. Xiao, Y. Cheng, W. Zhang, F. Huang, W. Zhang, H. Wang and B. Tang, *Chem. Commun.*, 2014, **50**, 7184-7187; (b) M. H. Lee, N. Park, C. Yi, J. H. Han, J. H. Hong, K. P. Kim, D. H. Kang, J. L. Sessler, C. Kang and J. S. Kim, *J. Am. Chem. Soc.*, 2014, **136**, 14136–14142.

8 K. W. Dunn, S. Mayor, J. N. Myers and F. R. Maxfield, *FASEB J.*, 1994, **8**, 573-582.

9 (a) M.Tantama, Y. P. Hung and G.Yellen, *J. Am. Chem. Soc.*, 2011, **133**, 10034–10037; (b) M. F. C. Abad, G. D. Benedetto, P. J. Magalhães, L. Filippin and T. Pozzan, *J. Biol. Chem.*, 2004, **279**, 11521–11529.

10 A. Takahashi, Y. Zhang, V. E. Centonze and B. Herman, *Biotechniques*, 2001, **30**, 804–815.

11 A. T. Hoye, J. E. Davoren, P. Wipf, M. P. Fink and V. E. Kagan, *Acc. Chem. Res.*, 2008, **41**, 87-97.

12 (a) Y. Chen, C. Zhu, Z. Yang, J. Chen, Y. He, Y. Jiao, W. He, L. Qiu, J. Cen and Z. Guo, *Angew. Chem. Int. Ed.*, 2013, **52**, 1688–1691; (b) F. Liu, T. Wu, J. F. Cao, S. Cui, Z. G. Yang, X. X. Qiang, S. G. Sun, F. L. Song, J. L. Fan, J. Y. Wang and X. J. Peng, *Chem. Eur. J.*, 2013, **19**, 1548–1553; (c) X. Wang, J. Sun, W. Zhang, X. Ma, J. Lv and B. Tang, *Chem. Sci.*, 2013, **4**, 2551-2556; (d) L. Yuan and Q.-P. Zuo, *Chem. Asian J.*, 2014, **9**, 1544-1549.

13 J. N. Demasa and G. A. Crosby, *J. Phys. Chem.*, 1971, **75**, 991-1024.

14 Z. Liu, C. Zhang, W. He, F. Qian, X. Yang, X. Gao and Z. Guo, *New J. Chem.*, 2010, **34**, 656-660.

15 (a) H. Mitsuhashi, S. Yamashita, H. Ikeuchi, T. Kuroiwa, Y. Kaneko, K. Hiromura, K. Ueki and Y.Nojima, *Shock*, 2005, **24**, 529-534; (b) M. Whiteman, J. S. Armstrong, S. H. Chu, S. Jia-Ling, B. S.Wong, N. S. Cheung and B. Halliwell, *J. Neurochem.*, 2004, **90**, 765-768.

16 K. L. Tsai, S. M. Wang, C. C. Chen, T. H. Fong and M. L. Wu, *J. Physiol.*, 1997, **502**, 161–174.

17 D. Srikun, E. W. Miller, D. W. Domaille and C. J. Chang, *J. Am. Chem. Soc.*, 2008, **130**, 4596–4597.